Hindawi
Journal of Advanced Transportation
Volume 2018, Article ID 9614501, 15 pages
https://doi.org/10.1155/2018/9614501

Research Article

Predicting Freeway Work Zone Capacity Distribution Based on Logistic Speed-Density Models

Chaoru Lu,[1] **Jing Dong**,[2] **Anuj Sharma**,[2] **Tingting Huang**,[2] **and Skylar Knickerbocker**[2]

[1]*Traffic Engineering Research Center, Department of Civil and Environmental Engineering, Norwegian University of Science and Technology, Trondheim, 7033, Norway*
[2]*Department of Civil, Construction and Environmental Engineering, Iowa State University, Ames, 50010, USA*

Correspondence should be addressed to Jing Dong; jingdong@iastate.edu

Received 3 April 2018; Revised 25 July 2018; Accepted 2 October 2018; Published 1 November 2018

Academic Editor: Maria Castro

Speed-volume-density relationship and capacity are key elements in modelling traffic operations, designing roadways, and evaluating facility performance. This paper uses a modified five-parameter logistic model to describe the speed-density relationship. The calibrated speed-density models show that the stop-and-go speed (V_b) and shape parameters (θ_1 and θ_2) are similar for work zones and the nonwork zone site. Accordingly, an operational capacity prediction method is proposed. To demonstrate the effectiveness of the proposed method, the predicted operational capacities are compared with the field data, Highway Capacity Manual method, the output of WorkZoneQ software, and the ensemble tree approach under different work zone scenarios. Furthermore, a lifetime distribution prediction framework for stochastic capacity of work zones is proposed. The predicted lifetime distribution can well capture the tendency of the observed work zone capacities.

1. Introduction

The conflict between the aged infrastructure and the continuous growth of traffic demand makes the maintenance and repair activities on roadways become commonplace. These activities usually cause traffic delays and safety concerns [1, 2]. Traffic control and management strategies, such as imposing reduced speed limits and coordinating lane closure schedules, have been applied to alleviate the impact of work zones [3–5]. To properly design work zone management strategies, accurate prediction of work zone capacity is crucial. Numerous statistical and simulation-based methods have been proposed to estimate or predict work zone capacity [3, 6–12]. However, only a few work zone capacity estimation methods were derived from speed-flow relationships [3, 10, 11], although speed, volume, and density relationship have been widely used to estimate the capacity of freeways [13].

Moreover, work zones usually induce bottlenecks and cause traffic breakdown. Traffic breakdown does not always occur at the maximum flow rate because of its stochastic nature [14, 15]. Therefore, predicting work zone capacity lifetime distribution, referred to as prebreakdown distribution in some literature, is crucial for transportation agencies to evaluate the traffic flow reliability at the work zone site. Several studies have investigated capacity distributions based on lifetime data analysis [14, 16, 17]. However, none of the existing methods focus on predicting work zone capacity lifetime distribution.

In this study, speed-volume-density relationships of both work zones and nonwork zone sites are developed. The work zone capacity is predicted based on the speed-volume-density models and the relationship between free-flow speed and work zone characteristics. The work zone capacity lifetime distribution is predicted based on the capacity distribution before work zone and work zone characteristics.

2. Literature Review

In the literature, the definition of capacity can be categorized into operational capacity and stochastic capacity [18, 19]. Operational capacity is usually derived from the maximum flow rate [20], the queue discharge rate [6, 9, 21], and the

speed-volume curve [11, 22, 23]. Queue discharge flow rate, which is measured after traffic breakdown, is generally lower than the sustaining flow rate before breakdown [24, 25]. Maximum flow rate is a single measurement and might be unreliable [24, 26]. The speed-volume curve is developed based on observations measured before and after traffic breakdown and describes the characteristics of traffic flow at the study site. Thus, the capacity derived from speed-volume curve is defined as the operational capacity in this paper. Furthermore, Kondyli et al. [24] and Highway Capacity Manual (HCM) 6th edition [27] recommended using prebreakdown flow rate as freeway capacity. However, previous research has shown that prebreakdown flow rates follow probability distributions [17, 19, 28]. In this paper, the distribution of prebreakdown flow rates is defined as stochastic capacity [18, 22].

Work zone operational capacity estimation and prediction methods can be categorized into three groups: simulation based, nonparametric, and parametric methods [2]. Microscopic traffic simulation models, such as CORSIM and VISSIM, have been applied to estimate the operational capacity of work zones with different lane closure configurations [29–31]. To replicate real world traffic conditions, the microscopic simulation models need to be calibrated to local conditions, which is usually a tedious and expensive procedure. Nonparametric methods, including neural-fuzzy logic, decision tree, and ensemble tree models, have been used to predict work zone operational capacity [12, 32, 33]. These nonparametric methods usually need extensive historical traffic data to provide reliable prediction. Parametric approaches use predetermined coefficients of the predictors that are calibrated based on the data collected from the work zone site to predict work zone operational capacity. For example, Krammes and Lopez [9] and Kim et al. [8] developed multiregression models to predict short-term work zone operational capacity. Al-Kaisy and Hall [6] and Al-Kaisy et al. [34] proposed a generic multiplicative model to predict the long-term work zone operational capacity based on the traffic data collected from Ontario, Canada. They investigated the effects of grade, the day of week, and weather condition on work zone operational capacity.

In addition, Highway Capacity Manual (HCM) 6th edition [27] proposed a method to calculate the work zone operational capacity. First, the work zone queues discharge rate is calculated as follows:

$$QDR_{wz} = 2093 - 154 \times f_{LCSI} - 194 \times f_{Br} - 179 \times f_{AT} + 9 \times f_{LAT} - 59 \times f_{DN} \quad (1)$$

where QDR_{wz} is the work zone queue discharge rate (pc/hr/ln); f_{LCSI} is the lane closure severity index, f_{LCSI} = *total number of lanes/number of open lanes*^{2}; f_{Br} is the barrier type, 0 for concrete, 1 for plastic cone or drum; f_{AT} is the area type, 0 for urban areas, 1 for rural areas; and f_{AT} is the lateral distance from the edge of travel lane adjacent to the work zone to the barrier, barricades, or cones; and f_{DN} is 1 for daytime, 0 for night time.

Since the unit of QDR_{wz} is passenger car per hour per lane, the capacity adjustment factor is applied to convert it to vehicle per hour per lane.

$$CAF_{MIX} = CAF_{AO} - CAF_T - CAF_G \quad (2)$$

where CAF_{MIX} is the mixed-flow capacity adjustment factor; CAF_{AO} is the capacity adjustment factor for the auto-only case, which defaults to 1.0; CAF_T is the capacity adjustment factor for the percentage of trucks in mixed-flow conditions, $CAF_T = 0.53 \times \text{Truck Percentage}^{0.72}$; and CAF_G is the capacity adjustment factor for grade for segment j in mixed-flow conditions, which is 0 in this study.

Therefore, the work zone operational capacity can be calculated as follows:

$$q_c = \frac{QDR_{wz}}{100 - \alpha_{wz}} \times 100 \times CAF_{MIX} \quad (3)$$

where α_{wz} is the percentage drop in capacity at the work zone due to queuing conditions (%). The recommended value is 13.4% for freeway work zone. q_c is the work zone operational capacity.

Over the years, several researchers tried to derive work zone operational capacity from speed-volume-density relationship to provide a reliable estimate [3, 10, 11, 35, 36]. Numerous models have been developed to describe the speed-volume-density relationship, including single-regime and multiregime models. Two parameter single-regime models, such as Greenshields model [37] and Newell's model [38], usually cannot fit traffic data under congested and uncongested conditions at the same time. Multiregime models, such as Edie model [39], modified Greenberg model [40], and the cluster analysis based model [41], use two or more curves to fit traffic data in different regimes separately. The main challenge of applying multiregime model is to determine breakpoints in a systematic way [42]. To overcome these limitations, MacNicholas [43] proposed a five-parameter logistic speed-density model, which can fit the congested and uncongested regimes using one curve. Wang et al. [42] pointed out that the five-parameter logistic speed-density model outperforms the three-parameter logistic speed-density model and the existing models, such as Greenshields model, Greenberg model, Modified Greenberg model, Van Aerde model, and Newell's model. Thus, the five-parameter logistic speed-density model is adopted in this paper to fit the traffic data collected at work zone sites.

Furthermore, work zone capacity distribution estimation and prediction methods have been introduced in recent years. For example, Weng and Yang [44] proposed a method to determine work zone capacity distribution based on probabilistic two-regime speed-flow relationships. Weng and Yan [45] developed a truncated lognormal distribution model to predict work zone capacity, where the distribution parameters are formulated as a linear function of work zone characteristics. Lu [46] proposed a framework to predict work zone capacity range based on single-regime speed-flow relationships. In addition, previous studies found that traffic flow breakdown occurs with some probability at various flow rates that are lower than the maximum flow rate, referred

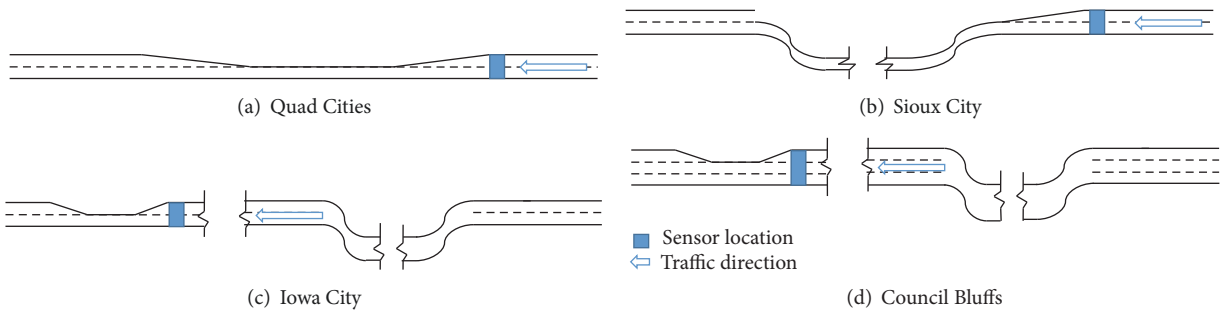

Figure 1: Work zone layouts.

to as stochastic capacity [14, 15, 47]. A lifetime distribution has been used to describe the probabilistic distribution of prebreakdown capacity. Different factors influencing freeway stochastic capacity have been investigated, including weather [17] and incidents [48]. In this study, the lifetime distribution is used to describe stochastic capacity of work zones.

In practice, HCS, QuickZone, QUEWZ, and WorkZoneQ are the commonly used software packages to estimate work zone operational capacity [49, 50]. In addition, the operational capacity estimation method proposed by Highway Capacity Manual 6th (HCM) [27] is also widely used by transportation agencies. In this paper, the results based on WorkZoneQ and HCM are compared with the proposed model. Moreover, the proposed model is compared with the work zone operational capacity prediction model proposed by Weng and Meng[12], which is based on the ensemble tree approach.

2.1. Objective and Contribution. The objective of this paper is to predict work zone operational capacity based on speed-volume-density relationship and predict the lifetime distribution of work zone capacity. The operational capacity prediction model captures the relationship between operational capacity and work zone characteristics, considering the impact of work zone on free-flow speed. The stochastic capacity is predicted based on the capacity distribution before work zone and work zone characteristics and is described using a Weibull distribution.

The contribution of this paper is two-fold. First, we propose a method to predict the speed-volume-density relationship and the operational capacity under work zone conditions by incorporating work zone characteristics in the five-parameter logistic speed-density model. Second, we propose a method to predict work zone capacity lifetime distribution considering the stochastic nature of flow breakdown. The proposed methods could help traffic engineers to predict work zone capacity and its distribution and design appropriate traffic management strategies to avoid long periods of oversaturation caused by work zones.

3. Data Description

Traffic flow rate, speed, and occupancy data were collected by Iowa Department of Transportation (DOT) using Wavetronix radar sensors placed in the work zone areas. Four work zones in Iowa during the 2015 and 2016 construction seasons are investigated in this study.

(i) Work zone data: Traffic volume, speed, and occupancy data were collected when the work zones were active in 2015 and 2016. The date and time of work zones are determined by combining traveler information data from Iowa DOT and the contractor reports and plans.

(ii) Baseline data: Traffic volume, speed, and occupancy data were collected from May to August in 2014 from the sensors located in the same or nearby locations of the work zone sites in Iowa City and Council Bluffs. Traffic data were also collected from May to August in 2015 at a freeway section in Des Moines where no work zone presented. These data are treated as the baseline for the work zones in Quad Cities and Sioux City because the Des Moines location has the same speed limit and similar geometric characteristic as the Quad Cities and Sioux City sites.

The configurations and layouts of the work zones are summarized in Table 1 and Figure 1, respectively. The sensors are located at the upstream of the merging area in order to measure prebreakdown flow rates [28, 51].

Based on the volume and speed measurements, the density is calculated using

$$k = \frac{q}{V} \tag{4}$$

where V is the speed (mi/h); k is the density (veh/mile/ln); and q is the volume (veh/hr/ln).

To focus on the traffic impact of work zones, the data collected on rainy days were removed. In addition, erroneous measurements were removed from the raw data. In particular, the average effective vehicle length (AEVL) is used to identify anomalies [52]. AEVL is calculated using speed, volume and occupancy collected from Wavetronix sensors [53], as shown in (5). The observations that result in AEVLs out of the normal vehicle length range, namely, 10 to 75 ft (3.048 to 22.86 m) [54], were removed from the dataset. The overall data reduction rate is 24.5%.

$$AEVL = \frac{5280 \times V \times O}{q} \tag{5}$$

Table 1: Summary of work zone configurations.

City	Work Zone	Truck Percentage	Speed limit (mph)		Work Type	Control Type	Barrier Type	Area Type	Work Time
			Original	Work zone					
Quad Cities	I80 WB	29.63%	65	55	Bridge deck overlay	Lane closure	Plastic Drum	Urban	Daylight
Quad Cities	I80 EB	29%	65	55	Bridge deck overlay	Lane closure	Plastic Drum	Urban	Daylight
Sioux City	I29 NB	13.24%	65	55	Pavement Reconstruction	Lane closure and shift	Plastic Drum	Urban	Daylight
Iowa City	I380 NB	15.97%	70	55	Bridge deck overlay	Lane closure /shift	Plastic Drum	Urban	Daylight
Council Bluffs	I80/I29 WB	17.23%	65	55	Road construction	Lane closure /shift	Concrete	Urban	Daylight

where AEVL is average effective vehicle lengths (feet); and O is the occupancy.

4. Methodology

4.1. Operational Capacity. According to MacNicholas' model [43], the function of general logistic speed-density relationship is expressed as

$$V = V_b + \frac{V_f - V_b}{\left(1 + \exp\left(\left(k - k_t\right)/\theta_1\right)\right)^{\theta_2}} \tag{6}$$

where V_f is the free-flow speed (mi/h); V_b is the average speed at stop-and-go condition (mi/h); k_t is the turning point that the speed–density curve transitions from free-flow to congested flow (veh/mi/ln); θ_1 is the scale parameter; and θ_2 is the parameter controls the lopsidedness of the curve.

By rearranging (6), traffic density can be written as follows:

$$k = k_t + \theta_1 \ln\left[\exp\left(\frac{\ln\left(\left(V_f - V_b\right)/\left(V - V_b\right)\right)}{\theta_2}\right) - 1\right] \tag{7}$$

where $\ln(\cdot)$ is the natural logarithm.

By substituting (7) into (4), the speed-volume function is derived as follows:

$$q = k_t V + \theta_1 \ln\left[\exp\left(\frac{\ln\left(\left(V_f - V_b\right)/\left(V - V_b\right)\right)}{\theta_2}\right) - 1\right] V \tag{8}$$

The relationship between turning point (k_t) and inflection point (k_{IP}) in the five-parameter logistic model is written in [42]

$$k_t = k_{IP} + \theta_1 \ln\left(\theta_2\right) \tag{9}$$

where k_{IP} is the inflection point, where the logistic speed-density curve switches from being concave to convex.

Wang et al. [42] pointed out that k_t has linear relationship with θ_1 and θ_2. In order to remove the collinearity between k_t and θ_1 and θ_2, α is introduced. In other words, k_t is written as a function of α, θ_1, θ_2, V_b, and V_f. When θ_2 equal 1, $k_t = k_{IP} = k_c$ [42]. Therefore, we assume

$$k_c = k_{IP} + \alpha\theta_1 \ln\left(\theta_2\right) \tag{10}$$

where k_c is the density at operational capacity (veh/mi/ln).

As a result,

$$V_c = V_b + \frac{V_f - V_b}{\left(1 + \theta_2^{\alpha-1}\right)^{\theta_2}} \tag{11}$$

where V_c is the speed at operational capacity (mi/h).

Using the speed-volume relationship, the operational capacity is reached when the following two conditions are met:

$$\frac{\partial q}{\partial V} = \frac{\partial k}{\partial V} \cdot V + k = 0 \tag{12}$$

$$\frac{\partial^2 q}{\partial V^2} = \frac{\partial k}{\partial V} + \frac{\partial^2 k}{\partial V^2} \cdot V + \frac{\partial k}{\partial V} < 0 \tag{13}$$

The derivations of the first condition and the second condition are shown in Appendix A.

Based on the first condition (i.e., (12)), the inflection density is derived as follows:

$$k_{IP} = \frac{\theta_1\left[V_b\left(1 + \theta_2^{\alpha-1}\right)^{\theta_2} + V_f - V_b\right]\left(1 + \theta_2^{\alpha-1}\right)}{\theta_2^{\alpha}\left(V_f - V_b\right)} - \alpha\theta_1 \ln\left(\theta_2\right) \tag{14}$$

As a result,

$$k_t = \frac{\theta_1\left[V_b\left(1 + \theta_2^{\alpha-1}\right)^{\theta_2} + V_f - V_b\right]\left(1 + \theta_2^{\alpha-1}\right)}{\theta_2^{\alpha}\left(V_f - V_b\right)} + (1 - \alpha)\,\theta_1 \ln\left(\theta_2\right) \tag{15}$$

The derivation of (14) is shown in Appendix B.

Therefore, the modified five-parameter logistic speed-density relationship and speed-volume relationship are shown as follows:

$$k = \frac{\theta_1\left[V_b\left(1 + \theta_2^{\alpha-1}\right)^{\theta_2} + V_f - V_b\right]\left(1 + \theta_2^{\alpha-1}\right)}{\theta_2^{\alpha}\left(V_f - V_b\right)} + (1 - \alpha)\,\theta_1 \ln\left(\theta_2\right) + \theta_1 \cdot \ln\left[\exp\left(\frac{\ln\left(\left(V_f - V_b\right)/\left(V - V_b\right)\right)}{\theta_2}\right) - 1\right] \tag{16}$$

$$q = \left[\frac{\theta_1\left[V_b\left(1 + \theta_2^{\alpha-1}\right)^{\theta_2} + V_f - V_b\right]\left(1 + \theta_2^{\alpha-1}\right)}{\theta_2^{\alpha}\left(V_f - V_b\right)} + (1 - \alpha)\,\theta_1 \ln\left(\theta_2\right) + \theta_1 \ln\left[\exp\left(\frac{\ln\left(\left(V_f - V_b\right)/\left(V - V_b\right)\right)}{\theta_2}\right) - 1\right]\right] \cdot V \tag{17}$$

Based on (15), the turning point changes with free-flow speed, average speed at stop-and-go condition, θ_1, θ_2, and α. θ_1 and θ_2 are the shape parameters of the speed-density curves. In this study, two assumptions are made:

(i) V_b, θ_1, and θ_2 remain the same during the work zone as the ones before work zone.

(ii) The same type of work zones has the same value of α.

From the second condition derived from (13), the exponential function is always greater than 0. Since θ_1 is positive, when $[\exp(\ln((V_f - V_b)/(V - V_b))/\theta_2) - 1] \times \theta_2 \times (V - 2V_b) + V$ is greater than 0, the condition stated in (13) is satisfied. As a result, we assume that

$$\left[\exp\left(\frac{\ln\left(\left(V_f - V_b\right)/\left(V_c - V_b\right)\right)}{\theta_2}\right) - 1\right] \times \theta_2 \times \left(V_c - 2V_b\right) + V_c > 0 \tag{18}$$

When $V_c \geq 2V_b$, the second condition is satisfied.

As a result, the operational capacity can be calculated as follows:

$$q_c = \max q, \quad V\epsilon\left[2V_b, V_f\right] \tag{19}$$

4.2. Stochastic Capacity. In previous research, flow breakdown is identified when speed drops from free-flow speed and the low speed is sustained for a certain time duration (i.e., minimum breakdown duration) [51, 55]. Accordingly, Kim et al. [17] proposed a criterion to classify breakdown and stochastic capacity, as follows:

If the speed in time interval i is above a threshold speed and the speed in the next time interval $i + 1$ is below the threshold speed, and the low speed is sustained for at least 15 min, breakdown is assumed to start in time interval $i + 1$, and the flow rate in time interval i is defined as the stochastic capacity.

According to Brilon et al. [51], when a breakdown occurred, the prebreakdown flow rate is considered a true estimate of stochastic capacity, which is a censored value. When the breakdown did not occur, the flow rates are created as uncensored values. Considering both the censored and the uncensored values, a survival analysis approach is applied to estimate the lifetime distribution of the capacity using the maximum likelihood estimation (MLE). The likelihood function is defined as follows [56]:

$$L = \prod_{i=1}^{n} f\left(q_i\right)^{\delta_i} \cdot \left[1 - F\left(q_i\right)\right]^{1-\delta_i} \tag{20}$$

where n is number of observations; δ_i is 1, if uncensored, and 0, otherwise; $f(\cdot)$ is probability density function; and $F(\cdot)$ is cumulative distribution function.

Weibull distribution has been calibrated and suggested for freeway reliability analysis by Al-Deek and Emam [57] and Brilon et al. [51] and is used to fit the observations in this paper.

$$F\left(q\right) = 1 - e^{-(q/\sigma)^s} \tag{21}$$

where σ is scale parameter; and s is shape parameter.

The mean of the stochastic capacity distribution is given by

$$E\left(q\right) = \sigma \cdot \Gamma\left(1 + \frac{1}{s}\right) \tag{22}$$

where $\Gamma(\cdot)$ is the gamma function.

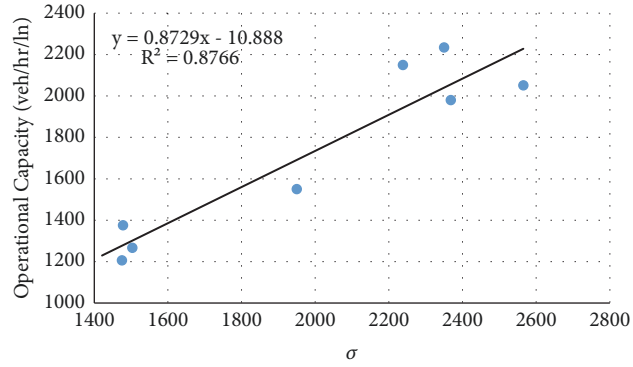

Figure 2: Relationship between the scale parameter and the operational capacity.

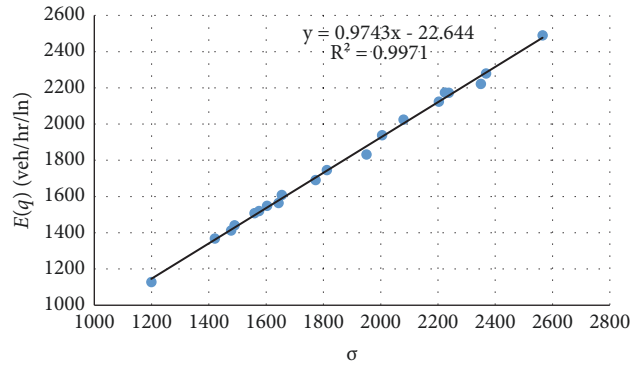

Figure 3: Relationship between the scale parameter and the mean capacity.

To investigate the relationship between the scale parameter and the operational capacity and the relationship between the scale parameter and the mean stochastic capacity, data from the study of [22] and the data collected in Iowa are summarized in Table 2. The mean of stochastic capacity is derived based on (22).

The relationship between scale parameter and operational capacity is plotted in Figure 2. The scale parameter and operational capacity is highly correlated, with an R-square of 0.88. As a result, the linear relationship between scale parameter (σ) and operational capacity is written as

$$q_c = A \cdot \sigma + B \tag{23}$$

where A, B are coefficients, which are 0.8729 and -10.888, respectively.

The relationship between mean stochastic capacity and σ is plotted in Figure 3. The scale parameter and the mean stochastic capacity is highly correlated, with an R-square of 0.99. Accordingly, the linear relationship between scale parameter (σ) and mean of stochastic capacity distribution is shown as follows:

$$E\left(q\right) = C \cdot \sigma + D \tag{24}$$

where, C, D are coefficients, which are 0.9743 and -22.644 respectively.

Table 2: Operational capacity, mean and parameters of capacity distribution from an existing study and field data.

Source	Location	s	σ	Operational capacity(veh/hr/ln)	$E(q)$ (veh/hr/ln)
Liu et al. (2011)	SR-91	7.55	1950	1550	1831
		17.68	2565	2051	2489
Iowa	I-35/80	17.96	2238	2150	2173
	I-29	13.43	2368	1980	2278
	I-380	8.63	2350	2235	2221
Work Zone	I80 WB	11.04	1478	1376	1412
	I80 EB	15.16	1503	1267	1452
	I29 NB	14.45	1475	1206	1423

Table 3: Parameters of logistic speed-density models.

Data Source		V_f(mi/h)	V_b(mi/h)	k_t (mi/h)	θ_1	θ_2	α
Non-work Zone		69.39	5.14	34.95	7.61	0.35	0.489
Work Zone	I80 WB	63.74	5.32	21.02	7.53	0.37	-0.263
	I80 EB	64.46	5.06	24.54	7.82	0.37	-0.274
	I29 NB	51.67	5.17	20.54	7.51	0.38	-0.289

According to (24) and (22), the relationship between the shape parameter (s) and the scale parameter (σ) is derived as follows:

$$s = \frac{1}{\Gamma^{-1}(0.97436 - (22.644/\sigma)) - 1} \tag{25}$$

4.3. Work Zone Capacity Distribution Prediction. The work zone capacity and its lifetime distribution prediction framework is proposed, as follows.

Step 1. Estimate the five-parameter logistic model and the capacity distribution using traffic data collected before work zones. The function "nls" in R statistics package [58] is utilized to fit the speed-density curve based on the traffic data.

Step 2. Determine the mean work zone free-flow speed based on HCM (2016):

$$\begin{aligned} V_f = {} & 9.95 + 33.49 \times f_{sr} + 0.53 \times f_s - 5.6 \times f_{LCSI} \\ & - 3.94 \times f_{Br} - 1.71 \times f_{DN} - 1.45 \times f_{Nr} \end{aligned} \tag{26}$$

where f_{sr} is the ratio of the normal speed limit to work zone speed limit; f_s is speed limit of work zone (mi/h); and f_{Nr} is the number of ramps within 3 miles (4.8 km) upstream and 3 miles (4.8 km) downstream.

Step 3. Determine α based on work zone type.

Step 4. Calculate the work zone operational capacity using Equation (17) and (19). In particular, V_b, θ_1, and θ_2 are determined in Step 1. α is determined in Step 3. The free-flow speed is determined in Step 2.

Step 5. Calculate the scale parameter of the work zone capacity distribution based on (23) and the operational capacity determined in Step 4.

Step 6. Calculate the shape parameter of the work zone capacity distribution based on (25) and the scale parameter from Step 5.

5. Results

5.1. Operational Capacity. The estimated traffic speed-volume-density relationships for different work zones are compared with the baseline non-work zone conditions. The calibrated parameters are summarized in Table 3.

Table 3 shows that free-flow speeds and turning density are smaller at the work zone sites compared to the ones at the nonwork zone site. The stop-and-go speed (V_b) and shape parameters (θ_1 and θ_2) are similar for work zones and non-work zone sites. Moreover, the values of α at work zone sites are significantly smaller than the one at the nonwork zone site. However, the values of α at different work zones are similar. Note that all the work zones considered in this study are lane closure ones. Other types of work zones might result in different α values. In the subsequent analysis, α of work zones is set as -0.27.

The speed-volume-density relationships before and after work zone started are compared in Figures 4 and 5. In order to investigate the relationship between work zone capacity and the free-flow speed, V_b, θ_1, and θ_2 that are calibrated based on the before work zone data are assumed to remain the same during the work zone. Based on the predicted free-flow speed, the predicted operational capacity is close to the capacity estimated from the work zone data. The predicted speed-volume-density relationship follows the pattern of the field data collected at work zone sites.

Additionally, the estimated and predicted operational capacities are compared with the capacity estimates by WorkZoneQ software, HCM, the maximum 15-minute flow rate, and the operational capacities predicted by the model proposed by Weng and Meng [12]. As shown in Table 4, the modified five-parameter logistic model generates similar

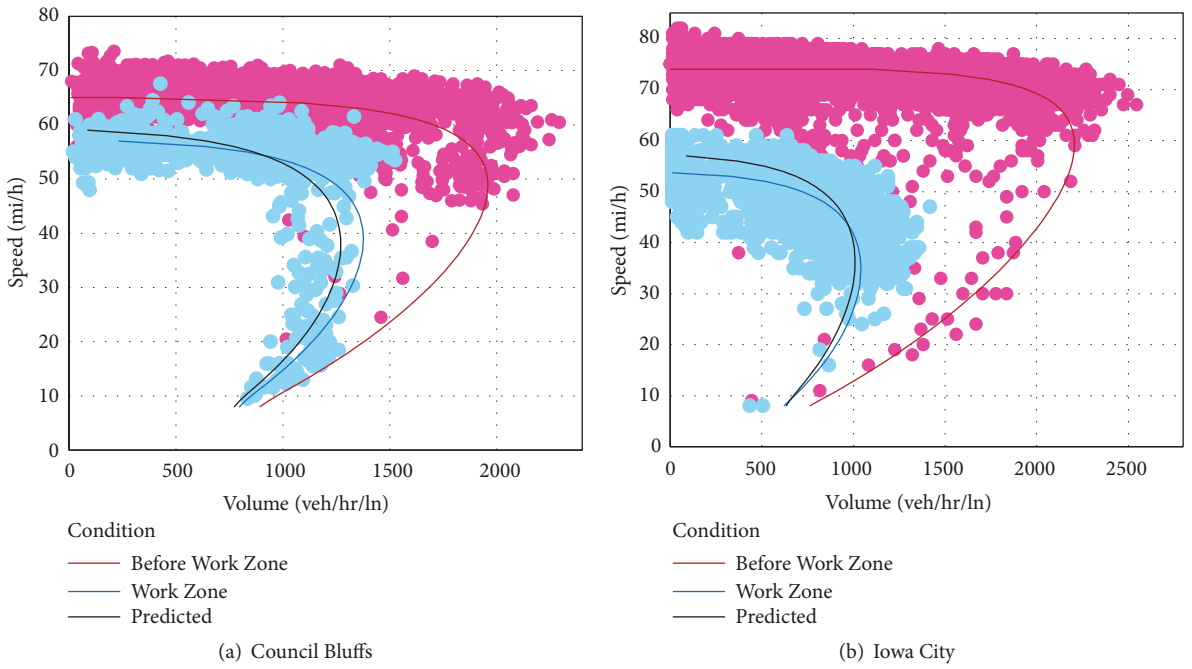

Figure 4: Speed-volume relationships before and during work zone.

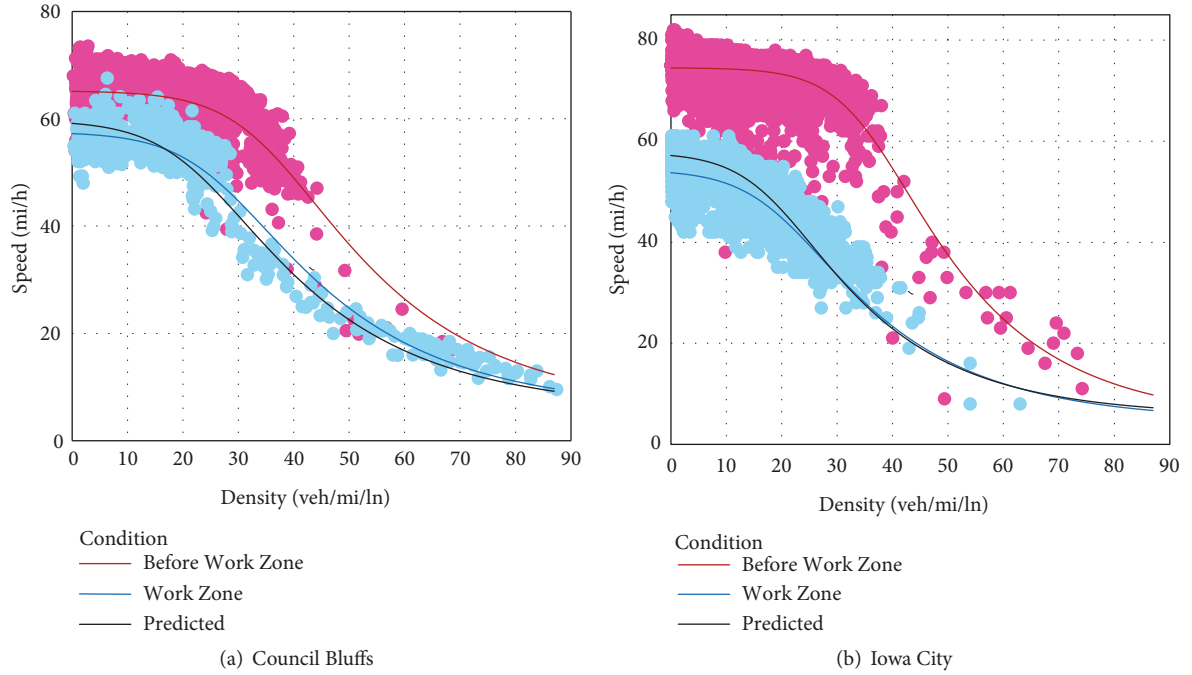

Figure 5: Speed-density relationships before and during work zone.

results as WorkZoneQ and HCM. The maximum 15-minute flow rate tends to overestimate capacity, compared to logistic model and WorkZoneQ results. The work zone in Iowa City, which has a larger free-flow speed reduction, has a lower operational capacity. The work zones that have similar free-flow speed reduction demonstrate similar capacities. Moreover, the predicted operational capacities based on the proposed method match the estimated values better than the Weng and Meng [12] method.

In Figure 6, the range of the predicted operational capacity of work zone (i.e., the shaded area) is compared with the results reported in the literature. The predicted capacities tend to be lower than the work zone operational capacities in the literature. One of the reasons is that maximum 15-min

Table 4: Operational capacities from the proposed method, HCM, Weng and Meng method [12], WorkZoneQ and maximum 15-minute flow rate.

City	Work Zone	Maximum 15-min flow rate (veh/hr/ln)	Estimated operational capacity (veh/hr/ln)			Predicted operational capacity (veh/hr/ln)	
			HCM	Logistic Model	WorkZoneQ	Proposed method	Weng and Meng[12]
Quad Cities	I80 WB	1572	1239	1267	1296	1252	1383
Quad Cities	I80 EB	1488	1245	1206	1296	1318	1383
Sioux City	I29 NB	1512	1394	1413	1313	1257	1138
Iowa City	I-380 NB	1296	1199	1058	1424	1008	1383
Council Bluffs	I80/I29 WB	1524	1517	1376	1313	1281	1138

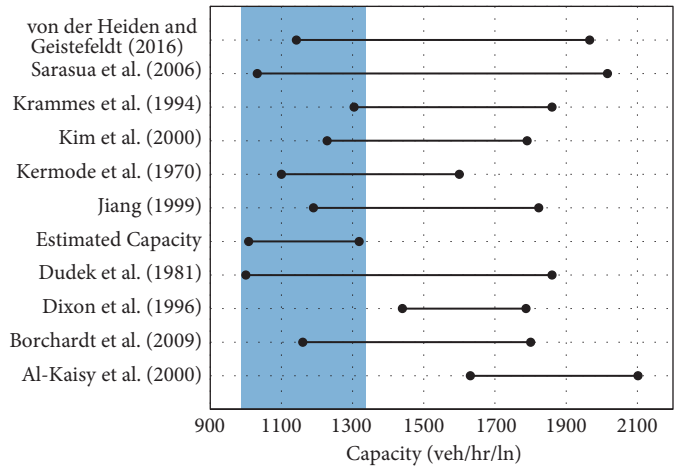

Figure 6: Comparison of the predicted capacity and the results from the existing studies.

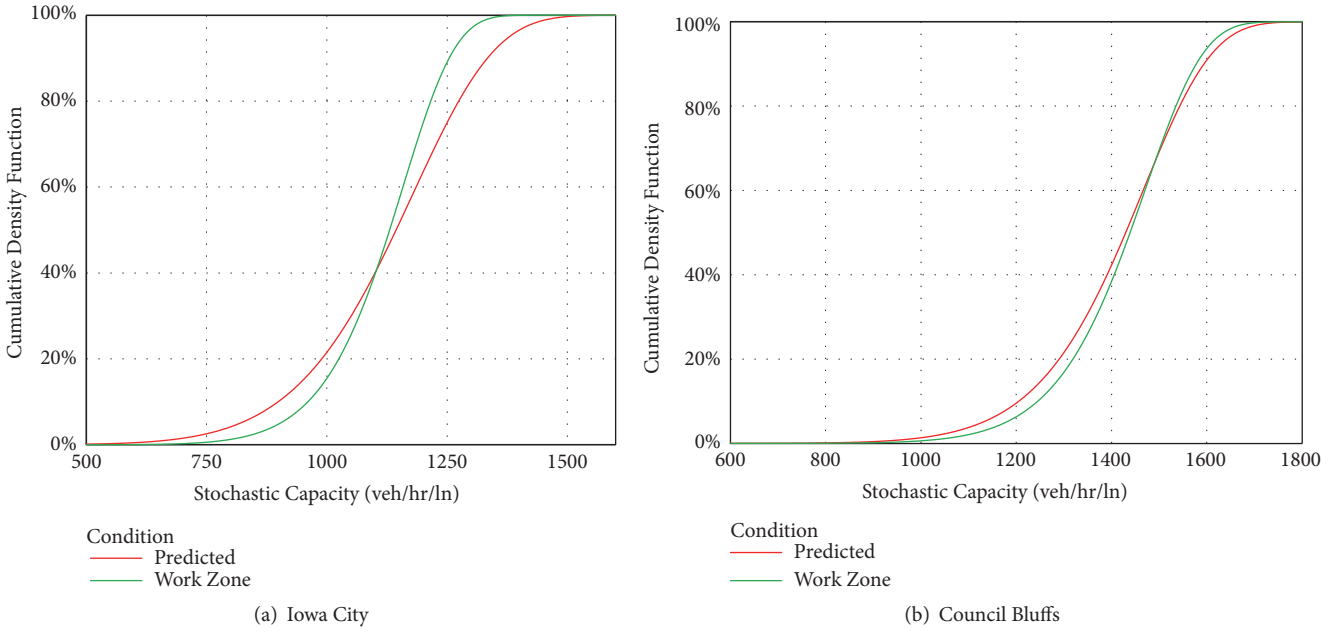

(a) Iowa City (b) Council Bluffs

Figure 7: Predicted and estimated stochastic capacity distributions.

flow rate was used as operational capacities in most of the previous studies.

5.2. Capacity Distribution. Based on the predicted operational capacity from Table 4, the scale parameter of work zone capacity lifetime distribution can be calculated. The parameters of stochastic capacity distributions before and during work zone started are shown in Table 5. The scale parameters of work zone are significantly smaller than the ones before work zone.

The predicted and estimated work zone stochastic capacity distribution are compared, as shown in Figure 7. The predicted work zone stochastic capacity distribution captured the tendency of the estimated work zone stochastic capacity distribution well.

Table 5: Parameters of Fitted and Predicted Distribution Functions.

City	Before		Work zone			
	Estimated		Estimated		Predicted	
	s	σ	s	σ	s	σ
Iowa City	8.64	2350	7.82	1199	11.56	1167
Council Bluffs	13.44	2368	11.04	1478	13.03	1480

The errors in the proposed capacity distribution prediction approach could be attributed to several factors. First, the difference between predicted operational capacity and the ground truth operational capacity may cause errors in predicting the scale parameter of work zone. Second, the data used to calibrate the relationship between scale parameter and shape parameter is limited.

6. Conclusions

The effects of work zones on traffic speed-volume-density curves and the roadway capacity are investigated using traffic data collected on freeways in Iowa, USA. A modified five-parameter logistic model is developed to describe the speed-density relationship. The calibrated speed-density models show that the free-flow speed and turning density are smaller when work zone is active compared to non-work zone conditions. Moreover, based on the logistic speed-density model, an operational capacity prediction method is proposed considering the relationship between free-flow speed and work zone characteristics. The performance of the proposed work zone capacity prediction method is evaluated using field data. The logistic model-based method can predict the speed-density relationship that is close to the estimated one from the field data. The predicted work zone operational capacities are similar to the results from WorkZoneQ and HCM and are generally smaller than the maximum 15-min flow rate. Moreover, the predicted operational capacities based on the proposed method is closer to the estimated values than the one proposed by Weng and Meng [12].

Furthermore, a work zone distribution prediction framework is proposed. Based on existing studies and the field data, a linear relationship between the scale parameter (σ) and the operational capacity is established. The predicted capacity distribution can well capture the tendency of the distribution estimated based on the field data.

There are some caveats in the present paper. First, only work zones with lane closure are considered in the study. In the future, other types of work zones need to be investigated. Second, only free-flow speed and α are considered as dependent variables that influence the speed-density curve. Future studies should examine the impact of work zone intensity, traffic control type, and road configuration on the other parameters of the logistic model. Third, the linear relationship between scale parameter (σ) and operational capacity is based on the limited data from existing studies and the field data. In the future, comprehensive datasets, including different impacting factors needs to be considered.

Appendix

A. Sufficient Conditions for Capacity

The First Condition

$$\frac{\partial k}{\partial V} = \theta_1 \times \frac{\partial}{\partial V}\left[\ln\left[\exp\left(\frac{\ln\left(\left(V_f - V_b\right)/\left(V - V_b\right)\right)}{\theta_2}\right) - 1\right]\right] \tag{A.1}$$

Derivation

$$\begin{aligned}
&\frac{\partial}{\partial V}\left[\ln\left[\exp\left(\frac{\ln\left(\left(V_f - V_b\right)/\left(V - V_b\right)\right)}{\theta_2}\right) - 1\right]\right] = \frac{1}{\exp\left(\ln\left(\left(V_f - V_b\right)/\left(V - V_b\right)\right)/\theta_2\right) - 1} \\
&\times \frac{\partial}{\partial V}\left[\exp\left(\frac{\ln\left(\left(V_f - V_b\right)/\left(V - V_b\right)\right)}{\theta_2}\right) - 1\right] = \frac{1}{\exp\left(\ln\left(\left(V_f - V_b\right)/\left(V - V_b\right)\right)/\theta_2\right) - 1} \\
&\times \frac{\partial}{\partial V}\left[\exp\left(\frac{\ln\left(\left(V_f - V_b\right)/\left(V - V_b\right)\right)}{\theta_2}\right)\right] = \frac{\exp\left(\ln\left(\left(V_f - V_b\right)/\left(V - V_b\right)\right)/\theta_2\right)}{\theta_2\left[\exp\left(\ln\left(\left(V_f - V_b\right)/\left(V - V_b\right)\right)/\theta_2\right) - 1\right]} \times \frac{\partial}{\partial V}\left[\ln\left(\frac{V_f - V_b}{V - V_b}\right)\right] \\
&= -\frac{\left(\left(V - V_b\right)/\left(V_f - V_b\right)\right) \times \exp\left(\ln\left(\left(V_f - V_b\right)/\left(V - V_b\right)\right)/\theta_2\right)}{\theta_2\left[\exp\left(\ln\left(\left(V_f - V_b\right)/\left(V - V_b\right)\right)/\theta_2\right) - 1\right]} \times \frac{\partial}{\partial V}\left[\frac{V_f - V_b}{V - V_b}\right] \\
&= -\frac{\left(V - V_b\right) \times \exp\left(\ln\left(\left(V_f - V_b\right)/\left(V - V_b\right)\right)/\theta_2\right)}{\theta_2\left[\exp\left(\ln\left(\left(V_f - V_b\right)/\left(V - V_b\right)\right)/\theta_2\right) - 1\right]} \times \frac{\partial}{\partial V}\left[\frac{1}{V - V_b}\right] \\
&= -\frac{\exp\left(\ln\left(\left(V_f - V_b\right)/\left(V - V_b\right)\right)/\theta_2\right)}{\left(V - V_b\right) \times \theta_2\left[\exp\left(\ln\left(\left(V_f - V_b\right)/\left(V - V_b\right)\right)/\theta_2\right) - 1\right]}
\end{aligned} \tag{A.2}$$

As a result,

$$\frac{\partial q}{\partial V} = k - \frac{\theta_1 \times V \times \exp\left(\ln\left(\left(V_f - V_b\right)/\left(V - V_b\right)\right)/\theta_2\right)}{\left(V - V_b\right) \times \theta_2\left[\exp\left(\ln\left(\left(V_f - V_b\right)/\left(V - V_b\right)\right)/\theta_2\right) - 1\right]} \tag{A.3}$$

As a result

$$\frac{\partial q}{\partial V} = k - \frac{V \times \exp\left(\ln\left(\left(V_f - V_b\right)/\left(V - V_b\right)\right)/\theta_2\right)}{\left(V - V_b\right) \times \theta_2\left[\exp\left(\ln\left(\left(V_f - V_b\right)/\left(V - V_b\right)\right)/\theta_2\right) - 1\right]} = 0 \tag{A.4}$$

The Second Condition

$$\frac{\partial^2 q}{\partial V^2} = -\frac{\theta_1 \times \exp\left(\ln\left(\left(V_f - V_b\right)/\left(V - V_b\right)\right)/\theta_2\right)\left[\left[\exp\left(\ln\left(\left(V_f - V_b\right)/\left(V - V_b\right)\right)/\theta_2\right) - 1\right] \times \theta_2 \times \left(V - 2V_b\right) + V\right]}{\left[\theta_2 \times \left(V - V_b\right)\right]^2 \times \left[\exp\left(\ln\left(\left(V_f - V_b\right)/\left(V - V_b\right)\right)/\theta_2\right) - 1\right]^2} \tag{A.5}$$

Derivation

$$\begin{aligned}
\frac{\partial^2 q}{\partial V^2} &= \theta_1 \times \frac{\partial}{\partial V}\left[\ln\left[\exp\left(\frac{\ln\left(\left(V_f - V_b\right)/\left(V - V_b\right)\right)}{\theta_2}\right) - 1\right]\right] - \theta_1 \\
&\times \frac{\partial}{\partial V}\left[\frac{V \times \exp\left(\ln\left(\left(V_f - V_b\right)/\left(V - V_b\right)\right)/\theta_2\right)}{\left(V - V_b\right) \times \theta_2\left[\exp\left(\ln\left(\left(V_f - V_b\right)/\left(V - V_b\right)\right)/\theta_2\right) - 1\right]}\right] \\
&= -\frac{\theta_1 \times \exp\left(\ln\left(\left(V_f - V_b\right)/\left(V - V_b\right)\right)/\theta_2\right)}{\left(V - V_b\right) \times \theta_2\left[\exp\left(\ln\left(\left(V_f - V_b\right)/\left(V - V_b\right)\right)/\theta_2\right) - 1\right]} - \theta_1 \\
&\times \frac{\partial}{\partial V}\left[\frac{V \times \exp\left(\ln\left(\left(V_f - V_b\right)/\left(V - V_b\right)\right)/\theta_2\right)}{\left(V - V_b\right) \times \theta_2\left[\exp\left(\ln\left(\left(V_f - V_b\right)/\left(V - V_b\right)\right)/\theta_2\right) - 1\right]}\right] \\
\frac{\partial}{\partial V}&\left[\frac{V \times \exp\left(\ln\left(\left(V_f - V_b\right)/\left(V - V_b\right)\right)/\theta_2\right)}{\left(V - V_b\right) \times \theta_2\left[\exp\left(\ln\left(\left(V_f - V_b\right)/\left(V - V_b\right)\right)/\theta_2\right) - 1\right]}\right] = \frac{1}{\theta_2} \\
&\times \frac{\partial}{\partial V}\left[\frac{V \times \exp\left(\ln\left(\left(V_f - V_b\right)/\left(V - V_b\right)\right)/\theta_2\right)}{\left(V - V_b\right) \times \left[\exp\left(\ln\left(\left(V_f - V_b\right)/\left(V - V_b\right)\right)/\theta_2\right) - 1\right]}\right] = \frac{1}{\theta_2} \\
&\times \left[\frac{(\partial/\partial V)\left[V \times \exp\left(\ln\left(\left(V_f - V_b\right)/\left(V - V_b\right)\right)/\theta_2\right)\right]}{\left(V - V_b\right) \times \left[\exp\left(\ln\left(\left(V_f - V_b\right)/\left(V - V_b\right)\right)/\theta_2\right) - 1\right]}\right. \\
&\left. - \frac{V \times \exp\left(\ln\left(\left(V_f - V_b\right)/\left(V - V_b\right)\right)/\theta_2\right) \times (\partial/\partial V)\left[\left(V - V_b\right) \times \left[\exp\left(\ln\left(\left(V_f - V_b\right)/\left(V - V_b\right)\right)/\theta_2\right) - 1\right]\right]}{\left(V - V_b\right)^2 \times \left[\exp\left(\ln\left(\left(V_f - V_b\right)/\left(V - V_b\right)\right)/\theta_2\right) - 1\right]^2}\right] \\
\frac{\partial}{\partial V}&\left[V \times \exp\left(\frac{\ln\left(\left(V_f - V_b\right)/\left(V - V_b\right)\right)}{\theta_2}\right)\right] = \exp\left(\frac{\ln\left(\left(V_f - V_b\right)/\left(V - V_b\right)\right)}{\theta_2}\right) \\
&+ \frac{\partial}{\partial V}\left[\exp\left(\frac{\ln\left(\left(V_f - V_b\right)/\left(V - V_b\right)\right)}{\theta_2}\right)\right] = \exp\left(\frac{\ln\left(\left(V_f - V_b\right)/\left(V - V_b\right)\right)}{\theta_2}\right) \\
&- \frac{V \times \exp\left(\ln\left(\left(V_f - V_b\right)/\left(V - V_b\right)\right)/\theta_2\right)}{\theta_2 \times \left(V - V_b\right)} \\
\frac{\partial}{\partial V}&\left[\left(V - V_b\right) \times \left[\exp\left(\frac{\ln\left(\left(V_f - V_b\right)/\left(V - V_b\right)\right)}{\theta_2}\right) - 1\right]\right] = \left[\exp\left(\frac{\ln\left(\left(V_f - V_b\right)/\left(V - V_b\right)\right)}{\theta_2}\right) - 1\right] \\
&- \frac{\exp\left(\ln\left(\left(V_f - V_b\right)/\left(V - V_b\right)\right)/\theta_2\right)}{\theta_2}
\end{aligned}$$

As a result,

$$\begin{aligned}
\frac{\partial^2 q}{\partial V^2} = \theta_1 \times \left[-\right.&\frac{V \times \exp\left(2\ln\left(\left(V_f - V_b\right)/\left(V - V_b\right)\right)/\theta_2\right)}{\left[\theta_2 \times \left(V - V_b\right)\right]^2 \times \left[\exp\left(\ln\left(\left(V_f - V_b\right)/\left(V - V_b\right)\right)/\theta_2\right) - 1\right]^2} \\
&\left. - \frac{2\exp\left(2\ln\left(\left(V_f - V_b\right)/\left(V - V_b\right)\right)/\theta_2\right)}{\theta_2 \times \left(V - V_b\right) \times \left[\exp\left(\ln\left(\left(V_f - V_b\right)/\left(V - V_b\right)\right)/\theta_2\right) - 1\right]}\right]
\end{aligned}$$

$$+\frac{V\times\exp\left(\ln\left(\left(V_f-V_b\right)/\left(V-V_b\right)\right)/\theta_2\right)}{\theta_2\times\left(V-V_b\right)^2\times\left[\exp\left(\ln\left(\left(V_f-V_b\right)/\left(V-V_b\right)\right)/\theta_2\right)-1\right]}$$

$$+\frac{V\times\exp\left(\ln\left(\left(V_f-V_b\right)/\left(V-V_b\right)\right)/\theta_2\right)}{\left[\theta_2\times\left(V-V_b\right)\right]^2\times\left[\exp\left(\ln\left(\left(V_f-V_b\right)/\left(V-V_b\right)\right)/\theta_2\right)-1\right]}\Bigg]$$

$$=-\frac{\theta_1\times\exp\left(\ln\left(\left(V_f-V_b\right)/\left(V-V_b\right)\right)/\theta_2\right)\left[\left[\exp\left(\ln\left(\left(V_f-V_b\right)/\left(V-V_b\right)\right)/\theta_2\right)-1\right]\times\theta_2\times\left(V-2V_b\right)+V\right]}{\left[\theta_2\times\left(V-V_b\right)\right]^2\times\left[\exp\left(\ln\left(\left(V_f-V_b\right)/\left(V-V_b\right)\right)/\theta_2\right)-1\right]^2} \tag{A.7}$$

B. Derivation of the Inflection Density

$$\frac{\partial q}{\partial V}=k_c-\frac{\theta_1\times V_c\times\exp\left(\ln\left(\left(V_f-V_b\right)/\left(V_c-V_b\right)\right)/\theta_2\right)}{\left(V_c-V_b\right)\times\theta_2\left[\exp\left(\ln\left(\left(V_f-V_b\right)/\left(V_c-V_b\right)\right)/\theta_2\right)-1\right]}=0 \tag{B.1}$$

By substituting (5) and (6) into it, we have

$$k_{IP}+\alpha\theta_1\ln\left(\theta_2\right)=\frac{\theta_1\times\left(V_b+\left(V_f-V_b\right)/\left(1+\theta_2^{\alpha-1}\right)^{\theta_2}\right)\times\exp\left(\ln\left(\left(1+\theta_2^{\alpha-1}\right)^{\theta_2}\right)/\theta_2\right)}{\left(\left(V_f-V_b\right)/\left(1+\theta_2^{\alpha-1}\right)^{\theta_2}\right)\times\theta_2\left[\exp\left(\ln\left(\left(1+\theta_2^{\alpha-1}\right)^{\theta_2}\right)/\theta_2\right)-1\right]} \tag{B.2}$$

As a result,

$$k_{IP}=\frac{\theta_1\left[V_b\left(1+\theta_2^{\alpha-1}\right)^{\theta_2}+V_f-V_b\right]\left(1+\theta_2^{\alpha-1}\right)}{\theta_2^{1/\alpha}\left(V_f-V_b\right)}-\alpha\theta_1\ln\left(\theta_2\right) \tag{B.3}$$

Data Availability

The data were provided by Iowa Department of Transportation.

Conflicts of Interest

The authors declare that they have no conflicts of interest.

Acknowledgments

This research is sponsored by the Iowa Department of Transportation. The views and opinions expressed are those of the authors and do not necessarily reflect the views of the sponsoring agency.

References

[1] R. Harb, E. Radwan, X. Yan, A. Pande, and M. Abdel-Aty, "Freeway work-zone crash analysis and risk identification using multiple and conditional logistic regression," *Journal of Transportation Engineering*, vol. 134, no. 5, pp. 203–214, 2008.

[2] J. Weng and Q. Meng, "Estimating capacity and traffic delay in work zones: an overview," *Transportation Research Part C: Emerging Technologies*, vol. 35, pp. 34–45, 2013.

[3] J. Weng and Q. Meng, "Incorporating work zone configuration factors into speed-flow and capacity models," *Journal of Advanced Transportation*, vol. 49, no. 3, pp. 371–384, 2015.

[4] Y. Hou, P. Edara, and C. Sun, "Speed limit effectiveness in short-term rural interstate work zones," *Transportation Letters*, vol. 5, no. 1, pp. 8–14, 2013.

[5] R. J. Porter and J. S. Wood, "Exploring endogeneity of macroscopic speed parameters: Empirical study during low volume conditions in construction work zones," *Transportation Letters*, vol. 5, no. 1, pp. 27–37, 2013.

[6] A. Al-Kaisy and F. Hall, "Guidelines for estimating capacity at freeway reconstruction zones," *Journal of Transportation Engineering*, vol. 129, no. 5, pp. 572–577, 2003.

[7] K. Heaslip, C. Louisell, and J. Collura, "Driver Population Adjustment Factors for Highway Capacity Manuals Work Zone Capacity Equation," in *Presented at 87th Annual Meeting of the Transportation Research Board*, DC, Washington, 2008.

[8] T. Kim, D. J. Lovell, M. Hall, and J. Paracha, "A New Methodology to Estimate Capacity for Freeway Work Zones," in *in 80th Annual Meeting of the Transportation Research Board*, DC, Washington, 2000.

[9] R. A. Krammes and G. O. Lopez, "Updated capacity values for short-term freeway work zone lane closures," *Transportation Research Record*, no. 1442, pp. 49–56, 1994.

[10] S. Racha, M. Chowdhury, W. Sarasua, and Y. Ma, "Analysis of work zone traffic behavior for planning applications," *Transportation Planning and Technology*, vol. 31, no. 2, pp. 183–199, 2008.

[11] W. A. Sarasua, W. J. Davis, M. A. Chowdhury, and J. H. Ogle, "Estimating interstate highway capacity for short-term work zone lane closures: Development of methodology," *Transportation Research Record*, no. 1948, pp. 45–57, 2006.

[12] J. Weng and Q. Meng, "Decision tree-based model for estimation of work zone capacity," *Transportation Research Record*, no. 2257, pp. 40–50, 2011.

[13] V. Modi, A. Kondyli, S. S. Washburn, and D. S. McLeod, "Freeway capacity estimation method for planning applications," *Journal of Transportation Engineering*, vol. 140, no. 9, Article ID 05014004, 2014.

[14] L. Elefteriadou, R. P. Roess, and W. R. McShane, "Probabilistic nature of breakdown at freeway merge junctions," *Transportation Research Record*, vol. 1484, pp. 80–89, 1995.

[15] B. Persaud, S. Yagar, and R. Brownlee, "Exploration of the breakdown phenomenon in freeway traffic," *Transportation Research Record*, no. 1634, pp. 64–69, 1998.

[16] M. S. Iqbal, M. Hadi, and Y. Xiao, "Predicting arterial breakdown probability: A data mining approach," *Journal of Intelligent Transportation Systems: Technology, Planning, and Operations*, vol. 21, no. 3, pp. 190–201, 2016.

[17] J. Kim, H. S. Mahmassani, and J. Dong, "Likelihood and duration of flow breakdown: Modeling the effect of weather," *Transportation Research Record*, no. 2188, pp. 19–28, 2010.

[18] S. C. Calvert, H. Taale, and S. P. Hoogendoorn, "Quantification of motorway capacity variation: Influence of day type specific variation and capacity drop," *Journal of Advanced Transportation*, vol. 50, no. 4, pp. 570–588, 2016.

[19] X. Wu, P. Michalopoulos, and H. X. Liu, "Stochasticity of freeway operational capacity and chance-constrained ramp metering," *Transportation Research Part C: Emerging Technologies*, vol. 18, no. 5, pp. 741–756, 2010.

[20] W. A. Sarasua, W. J. Davis, D. B. Clarke, J. Kottapally, and P. Mulukutla, "Evaluation of interstate highway capacity for short-term work zone lane closures," *Transportation Research Record*, no. 1877, pp. 85–94, 2004.

[21] T. Schnell, J. S. Mohror, and F. Aktan, "Evaluation of traffic flow analysis tools applied to work zones based on flow data collected in the field," *Transportation Research Record: Journal of the Transportation Research Board*, vol. 1811, no. 02, pp. 57–66, 2002.

[22] X. Liu, B. J. Schroeder, T. Thomson, Y. Wang, N. M. Rouphail, and Y. Yin, "Analysis of operational interactions between freeway managed lanes and parallel, general purpose lanes," *Transportation Research Record*, vol. 2262, pp. 62–73, 2011.

[23] W. H. K. Lam, M. L. Tam, X. Cao, and X. Li, "Modeling the effects of rainfall intensity on traffic speed, flow, and density relationships for urban roads," *Journal of Transportation Engineering*, vol. 139, no. 7, pp. 758–770, 2013.

[24] A. Kondyli, B. St. George, L. Elefteriadou, and G. Bonyani, "Defining, measuring, and modeling capacity for the highway capacity manual," *Journal of Transportation Engineering*, vol. 143, no. 3, 2017.

[25] Y. Jiang, "Traffic Capacity, Speed, and Queue-Discharge Rate of Indiana's Four-Lane Freeway Work Zones," *Transportation Research Record*, no. 1657, pp. 10–17, 1999.

[26] R. F. Benekohal, A.-Z. Kaja-Mohideen, and M. V. Chitturi, "Methodology for estimating operating speed and capacity in work zones," *Transportation Research Record*, no. 1883, pp. 103–111, 2004.

[27] *Highway Capacity Manual - A Guide for Multimodal Mobility Analysis*, D.C.: Transportation R.B. Washington, 6th edition, 2016.

[28] W. Brilon, J. Geistefeldt, and H. Zurlinden, "Implementing the concept of reliability for highway capacity analysis," *Transportation Research Record*, vol. 2027, no. 1, pp. 1–8, 2007.

[29] K. Heaslip, A. Kondyli, D. Arguea, L. Elefteriadou, and F. Sullivan, "Estimation of freeway work zone capacity through simulation and field data," *Transportation Research Record*, no. 2130, pp. 16–24, 2009.

[30] I. Chatterjee, P. Edara, S. Menneni, and C. Sun, "Replication of work zone capacity values in a simulation model," *Transportation Research Record*, vol. 2130, pp. 138–148, 2009.

[31] K. Heaslip, M. Jain, and L. Elefteriadou, "Estimation of arterial work zone capacity using simulation," *Transportation Letters*, vol. 3, no. 2, pp. 123–134, 2011.

[32] H. Adeli and X. Jiang, "Neuro-fuzzy logic model for freeway work zone capacity estimation," *Journal of Transportation Engineering*, vol. 129, no. 5, pp. 484–493, 2003.

[33] J. Weng and Q. Meng, "Ensemble tree approach to estimating work zone capacity," *Transportation Research Record*, no. 2286, pp. 56–67, 2012.

[34] A. Al-Kaisy, M. Zhou, and F. Hall, "New insights into freeway capacity at work zones: Empirical case study," *Transportation Research Record*, no. 1710, pp. 154–160, 2000.

[35] K. A. Avrenli, R. Benekohal, and H. Ramezani, "Determining Speed-Flow Relationship and Capacity for Freeway Work Zone with No Lane Closure," in *90th Annual Meeting of the Transportation Research Board*, 2011.

[36] N. Bharadwaj, P. Edara, C. Sun, H. Brown, and Y. Chang, "Traffic Flow Modeling of Diverse Work Zone Activities," *Transportation Research Record*, 2018.

[37] B. D. Greenshields, "A study of traffic capacity," *Highway Research Board*, vol. 14, pp. 448–477, 1934.

[38] G. F. Newell, "Nonlinear effects in the dynamics of car following," *Operations Research*, vol. 9, pp. 209–229, 1961.

[39] L. C. Edie, "Car-following and steady-state theory for noncongested traffic," *Operations Research*, vol. 9, no. 1, pp. 66–76, 1961.

[40] J. S. Drake, J. L. Schofer, and A. D. May Jr, "A Statistical Analysis of Speed-Density Hypothses in Vehicular Traffic Science," *Highway Research Record*, vol. no. 154, pp. 112–117, 1967.

[41] L. Sun and J. Zhou, "Development of multiregime speed-density relationships by cluster analysis," *Transportation Research Record*, no. 1934, pp. 64–71, 2005.

[42] H. Z. Wang, J. Li, Q.-Y. Chen, and D. Ni, "Logistic modeling of the equilibrium speed-density relationship," *Transportation Research Part A: Policy and Practice*, vol. 45, no. 6, pp. 554–566, 2011.

[43] M. J. MacNicholas, "A simple and pragmatic representation of traffic flow," in *Symposium on The Fundamental Diagram*, pp. 161–177, 2011.

[44] J. Weng and X. Yan, "New methodology to determine work zone capacity distribution," *Transportation Research Record*, vol. 2461, pp. 25–31, 2014.

[45] J. Weng and X. Yan, "Probability distribution-based model for work zone capacity prediction," *Journal of Advanced Transportation*, vol. 50, no. 2, pp. 165–179, 2016.

[46] C. Lu, *Estimate freeway travel time reliability under recurring and nonrecurring congestion*, 2017.

[47] W. Brilon, J. Geistefeldt, and H. Zurlinden, "Implementing the concept of reliability for highway capacity analysis," *Transportation Research Record*, vol. 2027, no. 1, pp. 1–8, 2008.

[48] B. Wright, Y. Zou, and Y. Wang, "Impact of Traffic Incidents on Reliability of Freeway Travel Times," *Transportation Research Record*, vol. 2484, no. 1, pp. 90–98, 2018.

[49] R. F. Benekohal, A.-Z. Kaja-Mohideen, and M. V. Chitturi, "Evaluation of construction work zone operational issues: capacity , queue , and delay," in *Publication ITRC FR 00/01-4. Illinois Transportation Research Center*, 2003.

[50] R. Benekohal and H. Ramezani, *WorkZoneQ User Guide for Two-Lane Freeway Work Zones*, 2013.

[51] W. Brilon, J. Geistefeldt, and M. Regler, "Reliability of Freeway Traffic Flow: A stochastic Concept of Capacity," in *Proceedings of the 16th International Symposium on Transportation and Traffic Theory*, pp. 125–144, 2005.

[52] T. Wells, E. Smaglik, and D. Bullock, "Implementation of Station Health Monitoring Procedures for ITS Sensors, Volume 1: Research Report," Purdue University FHWA/IN/JTRP-2006/40-1, 2008.

[53] Wavetronix, "Wavetronix SmartSensor HD User Guide," http://www.signalcontrol.com/tech_papers/wavetronix/SS125_HD_InstallGuide.pdf.

[54] E. Minge, S. Peterson, H. Weinblatt, B. Coifman, and E. Hoekman, *Loop-and Length-Based Vehicle Classification*, Publication MN/RC 2012-33. Minnesota Department of Transportation, 2012.

[55] J. Dong and H. S. Mahmassani, "Flow breakdown and travel time reliability," *Transportation Research Record*, no. 2124, pp. 203–212, 2009.

[56] J. F. Lawless, *Statistical Models and Methods for Lifetime Data*, John Wiley & Sons, New York, NY, USA, 2003.

[57] H. Al-Deek and E. B. Emam, "New methodology for estimating reliability in transportation networks with degraded link capacities," *Journal of Intelligent Transportation Systems: Technology, Planning, and Operations*, vol. 10, no. 3, pp. 117–129, 2006.

[58] *R Development Core Team, "R: A Language and Environment for Statistical Computing*, 2011.